BIOCHEMISTRY
including biophysical chemistry & molecular biology

Article

pubs.acs.org/biochemistry

Effects of Select Histidine to Cysteine Mutations on Transcriptional Regulation by *Escherichia coli* RcnR

Khadine A. Higgins,[†,∥] Heidi Q. Hu,[‡] Peter T. Chivers,[§,⊥] and Michael J. Maroney*[,†,‡]

[†]Department of Chemistry and [‡]Program in Molecular and Cellular Biology, University of Massachusetts, Amherst, Massachusetts 01003, United States

[§]Department of Biochemistry and Molecular Biophysics, Washington University School of Medicine, St. Louis, Missouri 63110, United States

Supporting Information

ABSTRACT: The RcnR metalloregulator represses the transcription of the Co(II) and Ni(II) exporter, RcnAB. Previous studies have shown that Co(II) and Ni(II) bind to RcnR in six-coordinate sites, resulting in derepression. Here, the roles of His60, His64, and His67 in specific metal recognition are examined. His60 and His64 correspond to ligands that are important for Cu(I) binding in the homologous Cu(I)-responsive metalloregulator, CsoR. These residues are known to be functionally important in RcnR transcriptional regulation. X-ray absorption spectroscopy (XAS) was used to examine the structure of bound cognate and noncognate metal ions, and *lacZ* reporter assays were used to assess the transcription of *rcnA* in response to metal binding in the three His → Cys mutations, H60C, H64C, and H67C. These studies confirm that both Ni(II) and Co(II) use His64 as a ligand. H64C-RcnR is also the only known mutant that retains a Co(II) response while eliminating the response to Ni(II) binding. XAS data indicate that His60 and His67 are potential Co(II) ligands. The effects of the mutations of His60, His64, and His67 on the structures of the noncognate metal ions [Zn(II) and Cu(I)] reveal that these residues have distinctive roles in binding noncognate metals. None of the His → Cys mutants in RcnR confer any response to Cu(I) binding, including H64C-RcnR, where the ligands involved in Cu(I) binding in CsoR are present. These data indicate that while the secondary, tertiary, and quaternary structures of CsoR and RcnR are quite similar, small changes in primary sequence reveal that the specific mechanisms involved in metal recognition are quite different.

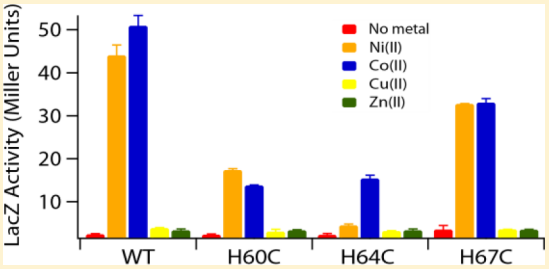

Transition metal ions are essential cofactors for many enzymes and proteins that carry out a variety of processes.[1] Excessively high concentrations of these metal ions can have severe effects on cellular metabolism.[2] For this reason, the levels of metal ions in cells need to be tightly regulated. Cellular trafficking systems for transition metals are equipped with importers, exporters, chaperones, and accessory proteins involved in metallocenter assembly, and transcriptional regulators that respond to specific transition metals. It is essential for trafficking systems to be selective with respect to their cognate metals to generate a metal-specific biological response.

The nickel trafficking pathway in *Escherichia coli* supplies nickel for hydrogenase active site assembly[3,4] and consists of the importer NikABCDE,[5,6] a nickel metallochaperone (HypA)[7,8] and other proteins that bind nickel and are involved in hydrogenase active site assembly (e.g., HypB and SlyD),[7,9,10] and an exporter RcnAB.[11−13] Two transcriptional regulators, NikR[14,15] (for NikABCDE) and RcnR[16] (for RcnAB), work together to regulate the expression of the importer and the exporter and to maintain nickel homeostasis.[16] Genetic studies published by Iwig et al.[16] indicate that RcnA is important for H_2ase3 activity by modulating NikR activity. RcnR and CsoR, a copper-responsive transcriptional regulator that represses *cso* that encodes a P-type ATPase for efflux of copper and a gene of unknown function, constitute a new structural class of transcriptional regulators characterized by an all-α-helical structure in a four-helix bundle.[17,18] *E. coli* RcnR is a 40 kDa tetrameric nickel- and cobalt-responsive transcriptional repressor.[16] The apoprotein recognizes a TACT-G_6-N-AGTA DNA motif, of which there are two located in the *rcnA*−*rcnR* intergenic region.[19] Apo-RcnR binds to DNA repressing the transcription of *rcnAB*, the genes encoding nickel and cobalt efflux proteins, RcnAB.[11] RcnR also interacts with flanking DNA regions of ∼50 bp, leading to DNA wrapping.[19] DNA binding is disfavored by the binding of 1 equiv of Ni(II) or Co(II) to RcnR, four per tetramer,[16,20] allowing for the transcription of the RcnAB exporter under conditions of excess metal. In addition to controlling the transcription of *rcnAB*, RcnR also controls the transcription of its own gene,[19,20] as does CsoR.[17]

The structurally related copper-responsive metalloregulator, CsoR, has been crystallographically characterized as an apoprotein from *Thermus thermophilus*[21] and *Streptomyces*

Received: July 2, 2012
Revised: December 6, 2012
Published: December 7, 2012

   dx.doi.org/10.1021/bi300886q | *Biochemistry* 2013, 52, 84−97

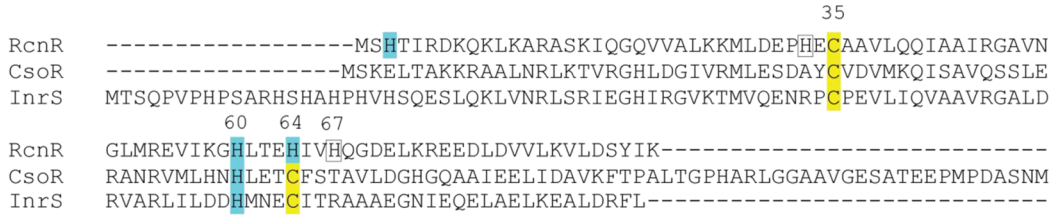

Figure 1. Sequence alignment of *E. coli* RcnR, *M. tuberculosis* CsoR, and *Synechocystis* PCC 6803 InrS generated using ClustalW.[27] The metal binding residues of RcnR and CsoR are highlighted as well as the corresponding residues in InrS. The additional histidine residues in RcnR are boxed.

lividans[22] as well as a Cu(I) complex using protein from *Mycobacterium tuberculosis*.[17] These structures show that the protein adopts an all-α-helical dimer of dimers quaternary structure. In the complex, Cu(I) is coordinated by two cysteine residues, Cys36 from one subunit and Cys65 from another subunit, as well as a histidine residue, His61, from the same subunit as Cys65.[17] Binding of Cu(I) to CsoR weakens the interaction between CsoR and the operator–promoter region of the *cso* operon,[17] presumably by disfavoring the DNA binding conformation. However, in the absence of a structure of the DNA complex, the details of how this occurs are unknown. Recently, a new member of the CsoR/RcnR family of proteins, InrS, was discovered in *Synechocystis* PCC 6803.[23] InrS is a Ni(II)-responsive transcriptional regulator that represses the transcription of *nrsD*, which encodes a Ni(II) efflux protein.[23] InrS binds Co(II), Ni(II), and Cu(I) and contains the Cu(I) binding ligands found in CsoR (Figure 1). However, InrS is responsive to the binding Ni(II), but not to Cu(I) binding. UV–vis data determined that the Ni site is four-coordinate with planar geometry,[23] and is more similar to the metal site structure of CsoR than RcnR.[23−26]

There is no crystal structure of RcnR, but data regarding the metal site structures obtained from XAS studies have established that the details of the metal binding are distinct from those of CsoR.[24,25] RcnR forms six-coordinate $M(N/O)_5S$ complexes with its cognate metal ions [Ni(II) and Co(II)], employing the single Cys that is conserved in the RcnR family of proteins (Cys35, homologous with Cys36 in CsoR) to bind both cognate metals.[24] Noncognate metal ions [e.g., Cu(I) and Zn(II)] are bound to RcnR by three protein ligands with an $(N/O)_2S$ donor atom set and may also incorporate an anion from the buffer.[25] One of the ligands missing from the noncognate sites is the N-terminal amine, which is bound to both cognate metals, or the side chain of His3, which is a ligand for only Co(II).[25] The Co(II) and Ni(II) sites are therefore distinguished by their histidine coordination, as well as by the M–S bond distance [2.31 Å for Co(II) vs 2.62 Å for Ni(II)].[24,25] *E. coli* RcnR possesses five histidine residues: His3, His33, His60, His64, and His67 (Figure 1). All five histidine residues were mutated by Iwig et al.,[24] who showed using a *lacZ* reporter assay that the three conserved residues in RcnR, His3, His60, and His64, are required for full sensitivity to Co(II) binding, while only His3 and His64 were required for full sensitivity to Ni(II) binding. The mutations of the nonconserved His33 and His67 had no significant effect on either the Co(II) or Ni(II) transcriptional response in cells.[24] However, these functional studies do not distinguish whether these His residues directly coordinate cognate or noncognate metals or which His residues might bind only to certain metals as all of these mutations involved side chains that are not expected to coordinate metals (Ala, Leu, Asn, or Arg).[24] To gain improved insight into Ni(II), Co(II), and noncognate metal binding, His → Cys mutations were introduced with the expectation that the additional S donor ligand would be apparent in the EXAFS spectrum if the substituted His residue is indeed a ligand. Additionally, CsoR possesses one His ligand and two Cys ligands that are used to coordinate Cu(I), so it is possible that a change in metal recognition might be promulgated by creating the Cu(I) ligand set of CsoR in RcnR (the H64C mutant). The metal site structures for Co(II), Ni(II), Cu(I), and Zn(II) complexes of the mutant proteins were then characterized using XAS, and the response of the mutant proteins to various metal ions was determined by using *lacZ* reporter assays. These studies provide additional insight into the role of His ligation in cognate and noncognate metal complexes, although surprisingly the mutant proteins failed to produce a Cu(I) sensor or even CsoR-like Cu(I) coordination, indicating that there is more complexity to metal responsiveness besides the coordination number, ligands employed, and their position in the protein amino acid sequence even in this simple helical bundle structural scaffold.

EXPERIMENTAL PROCEDURES

RcnR Mutagenesis. Point mutations of His60, His64, or His67 to Cys were introduced into the wild-type RcnR plasmid[24] using the QuikChange site-directed mutagenesis kit (Stratagene). Primers used in the polymerase chain reactions (PCRs) are listed in Table S1 of the Supporting Information. The PCR product was transformed into NovaBlue (Novagen) competent cells. The cells were then grown on LB/agar plates overnight, and a single colony was selected and grown overnight in a 5 mL culture (LB amp medium). The DNA was isolated using the Qiagen miniprep kit and sequenced at GENEWIZ Inc. (South Plainfield, NJ) to confirm that the correct mutation was present.

RcnR Overexpression and Purification. Single colonies of *E. coli* DL41(DE3) pLysS cells containing the plasmid encoding H60C-, H64C-, and H67C-RcnR mutant proteins were grown in 150 mL of Luria-Bertani broth (LB) cultures, supplemented with 30 μg/mL cam and 100 μg/mL amp overnight at 37 °C while being shaken. An aliquot (20 mL) of the overnight culture was added to 2 L of fresh LB with cam and amp. The cultures were grown to an OD_{600} of ∼0.8 and then induced by addition of IPTG to a final concentration of 0.8 mM. The cells were harvested after 3 h by centrifugation (5000 ×*g* for 8 min), resuspended in residual medium, and frozen at −80 °C. The cells were lysed upon being thawed in a water bath at 37 °C and treated with 10 μL of a DNase I solution (10 mg/mL DNase I and 40% glycerol), 1.5 mM (final concentration) PMSF (MP Biomedicals), and 5 mM (final concentration) TCEP (Thermo Scientific). The mixture was then incubated at 37 °C for 0.5 h.

All chromatographic purifications employed an AKTA-FPLC system (Amersham Biosciences) and were conducted at room

dx.doi.org/10.1021/bi300886q | *Biochemistry* 2013, 52, 84−97

temperature. The lysed cells were centrifuged (~6000 ×*g* for 30 min), and the lysate was applied to a SP Sepharose column (18 mL) equilibrated with 20 mM Hepes (pH 7.0), 1 mM TCEP, 5 mM EDTA, 10% glycerol, and 50 mM NaCl (buffer A). The column was washed with 50 mL of buffer A followed by a linear gradient from 0 to 100% buffer B [20 mM Hepes (pH 7.0), 1 mM TCEP, 5 mM EDTA, 10% glycerol, and 1 M NaCl], in a total volume of 117 mL at a flow rate of 2 mL/min while 5 mL fractions were collected. A sodium dodecyl sulfate−polyacrylamide gel electrophoresis (SDS−PAGE) was used to determine the fractions containing RcnR; RcnR eluted between ~35 and 55% buffer B. These fractions were combined, concentrated to 4 mL, and loaded on a HiLoad 16/60 Superdex 200 (GE Life Sciences) column equilibrated with buffer C [20 mM Hepes (pH 7.0), 1 mM TCEP, 5 mM EDTA, 10% glycerol, and 300 mM NaCl]. One column volume (120 mL) of buffer C was run over the column at a flow rate of 0.7 mL/min, and fractions were collected on the basis of the absorbance at 280 nm. Protein fractions with an absorbance of >10 mAU were collected in 2 mL fractions. Following this column, SDS−PAGE was used to identify the fractions that contained RcnR; RcnR eluted as a single peak at a volume consistent with that of a tetramer. These RcnR fractions were concentrated and buffer-exchanged into buffer A. A MonoS 5/50 GL column (GE Life Sciences) was equilibrated with buffer A before 20 mL of the protein was loaded in buffer A. The column was washed with 20 mL of buffer A, followed by a linear gradient of 0 to 100% buffer B over 40 mL at a flow rate of 1.5 mL/min while 2 mL fractions were collected. The purity of the fractions was checked using SDS−PAGE; RcnR eluted as a single peak at ~15−30% buffer B. Pure fractions of RcnR were pooled together and stored at 4 °C. Molecular weights of the expressed proteins were determined by electrospray ionization mass spectrometry (ESI-MS) using a Bruker Esquire instrument equipped with an HP-HPLC system (Agilent) for the removal of salt present in the protein solutions. The molecular weight of expressed proteins was determined by ESI-MS and confirms the presence of the His → Cys mutation in each case (the calculated mass for each is 9969 Da; the masses obtained from mass spectrometry were 9967 Da for H60C-RcnR, 9967 Da for H64C-RcnR, and 9970 Da for H67C-RcnR). The molecular masses obtained are also consistent with the loss of the N-terminal methionine residue, as seen for the wild-type protein and all the previously characterized mutations.[24,25]

Metal Complexes of RcnR Proteins. The proteins were concentrated to ~150 μM and desalted twice using a buffer containing 20 mM Hepes (pH 7.0), 10% glycerol, and 300 mM NaBr, NaCl, or NaOAc salt (buffer M) using Zebra spin desalting columns, with a 7K molecular weight cutoff, in a volume of 10 mL (Pierce) to remove EDTA and TCEP. In the case of the Cu(I) samples, the final buffer also contained 2 mM TCEP. A buffer containing either NaOAc or NaCl was used in some cases to confirm the binding of exogenous buffer ligands. The protein concentrations were determined by using the experimentally determined extinction coefficient ε_{276} of 2530 M^{-1} cm^{-1} from protein denatured with 8 M guanidine hydrochloride.[24] Two to three equivalents of 10 mM aqueous stock solutions of $CoCl_2 \cdot 6H_2O$, $NiCl_2 \cdot 6H_2O$, $Zn(CH_3COO)_2 \cdot 2H_2O$, $Cu(CH_3COO)_2 \cdot H_2O$ (Fisher Scientific), or $[(CH_3CN)_4Cu]PF_6$ (Aldrich) salts was then added to the RcnR solutions to prepare the respective complexes. These samples were allowed to equilibrate overnight before being incubated with Chelex beads for ~30 min to remove any nonspecifically bound metal ions.

Cu(I)-RcnR was prepared under anaerobic conditions. Air was removed from the protein solution on a Schlenk line by alternating between argon and vacuum five times. The protein was then placed into a Coy (Coy Laboratory Products Inc., Grass Lakes, MI) anaerobic chamber (90% N_2 and 10% H_2) and incubated with 3 equiv of a 10 mM $(CH_3CN)_4CuPF_6$ solution (nitrogen-saturated anaerobic solution of 10% acetonitrile in water) overnight. Chelex beads were added to the solution to remove any nonspecifically bound metal ions. The oxidation states of the Cu(I) samples were verified using X-band EPR (Bruker ELEXSYS E-500 X-band spectrometer) at 77 K on the samples frozen in XAS holders and inserted into a finger dewar. The percentage of Cu(II) present in the sample was determined by comparing the second integrals of the Cu(I) protein spectra with that of a 1.03 mM Cu(II)-EDTA sample used as a standard. The Cu(I)-H60C-RcnR sample in buffer M with NaBr and the Cu(I)-H64C-RcnR sample in buffers with NaBr and NaCl had <1% Cu(II) present, while Cu(I)-H67C-RcnR in buffer M with NaBr had ~1.6% Cu(II) present (Figure S1 of the Supporting Information).

On the basis of the previously determined protein concentrations, samples of RcnR proteins containing ~1 ppm of the respective metals were prepared for metal analysis by diluting aliquots of the metal complexes to 1 mL with deionized water. The metal content was determined using a Perkin-Elmer Optima DV4300 ICP-OES instrument. The metal:protein ratios for samples prepared in buffer M with NaBr were as follows: H60C-RcnR, 0.84:1 with Co(II), 1.17:1 with Ni(II), 1.05:1 with Cu(I), and 1.17:1 with Zn(II); H64C-RcnR, 1.26:1 with Co(II), 0.59:1 with Ni(II), 1.33:1 with Cu(I), and 1.21:1 with Zn(II); H67C-RcnR, 0.935:1 with Co(II), 1.21:1 with Ni(II), 1.03:1 with Cu(I), and 1.05:1 with Zn(II). Complexes of H64C-RcnR in buffer M with NaCl had the following metal:protein ratios: 0.87:1 with Co(II), 0.76:1 with Ni(II), and 1.29:1 with Cu(I). A sample of Zn(II)-RcnR was made in buffer M with 300 mM NaOAc and a metal:protein ratio of 0.95:1. Metal complexes of H60C- and H67C-RcnR proteins in buffer M with NaOAc had the following metal:protein ratios: H60C-RcnR, 1.10:1 with Ni(II) and 1.00:1 with Zn(II); H67C-RcnR, 1.125:1 with Ni(II) and 0.70:1 with Zn(II).

***β*-Galactosidase Reporter Experiments.** *β*-Galactosidase reporter experiments were conducted using two plasmids as follows.[24] The chloramphenicol-resistant P_{rcnA}-*lacZ* plasmid, pJI115,[16] was transformed into *E. coli* strain PC888 (Δ*lacZ* Δ*rcnR*) after which ampicillin-resistant plasmids expressing the H60C-, H64C-, or H67C-RcnR protein were transformed into the strain. This strain background provides for low-level expression of the RcnR proteins. To assay reporter activity, the transformed cells were grown anaerobically in medium containing ampicillin and chloramphenicol with metals added at the maximal concentration for Ni(II), Co(II), Cu(II), Zn(II), or Cd(II) that resulted in <10% inhibition of growth (measured by the final OD_{600}): 500 μM $NiCl_2$, 150 μM $CoCl_2$, 100 μM $CuCl_2$, 300 μM $ZnCl_2$, and 50 μM $CdSO_4$.[24]

X-ray Absorption Spectroscopy (XAS). Samples of the metalated proteins were concentrated to 1−3.2 mM (50 μL) in 20 mM Hepes (pH 7.0) and 300 mM NaBr, NaCl, or NaOAc with 10% glycerol using a microspin concentrator (Vivascience). The samples were injected via syringe into polycarbonate XAS holders that were wrapped in kapton tape and rapidly frozen in liquid nitrogen. The final concentration

dx.doi.org/10.1021/bi300886q | *Biochemistry* 2013, 52, 84−97

and freezing of Cu(I)-RcnR were conducted under an anaerobic atmosphere in a Coy chamber.

XAS data for the RcnR protein samples were collected as previously described.[28] Data were collected under dedicated ring conditions on beamline X3b at the National Synchrotron Light Source (NSLS), Brookhaven National Laboratories (Upton, NY), with the exception of H67C-RcnR with Ni in buffer M with NaOAc, which was collected on beamline 9-3 at Stanford Synchrotron Radiation Laboratory (SSRL). For data collection at NSLS, each sample was injected via syringe into polycarbonate sample holders that were wrapped in kapton tape and frozen in liquid nitrogen. The samples were loaded into an aluminum sample holder, which was cooled to ∼50 K using a He displex cryostat. Data were collected under ring conditions of 2.8 GeV and 120−300 mA using a sagittally focusing Si(111) double-crystal monochromator. Harmonic rejection was accomplished with a Ni-coated focusing mirror. X-ray fluorescence was collected using a 13-element Ge detector (Canberra). Scattering was minimized by placing a Z-1 filter between the sample chamber and the detector. Additionally, for H64C-RcnR with Ni(II), H64C-RcnR with Zn(II), and H67C-RcnR with Zn(II) in buffer M containing NaCl, NaOAc, and NaOAc, respectively, data were collected at NSLS using a 30-element fluorescence detector (Canberra). At SSRL, data were collected at 10 K using a liquid helium cryostat (Oxford Instruments). The ring conditions were 3 GeV and 80−100 mA. Beamline optics consisted of a Si(220) double-crystal monochromator and two rhodium-coated mirrors, a flat mirror before the monochromator for harmonic rejection and vertical columnation, and a second toroidal mirror after the monochromator for focusing. X-ray fluorescence was collected using a 100-element detector (Canberra). Soller slits with a Z-1 element filter were placed between the sample chamber and the detector to minimize scattering.

XANES was collected from −200 to 200 eV relative to the metal edge. The X-ray energy for each metal K_α-edge was internally calibrated to the first inflection point of the corresponding metal foil: Co, 7709.5 eV; Ni, 8331.6 eV; Cu, 8980.3 eV; Zn, 9660.7 eV. EXAFS was collected to 13.5−16k above the edge energy (E_o), depending on the signal:noise ratio at high k values.

Data Reduction and Analysis. The XAS data reported are the average of 4−10 scans. Each XANES spectrum used in the average was analyzed for edge energy shifts that might indicate redox in the beam. None of the samples showed any significant changes. XANES and EXAFS data were analyzed using EXAFS123[29] and SixPack,[30] respectively. The SixPack fitting software builds on the ifeffit engine.[31,32] XANES analysis was conducted as described previously[28] by fitting a cubic function to the baseline in the pre-edge region of the spectra and using a 75% Gaussian and 25% Lorenzian function to fit the rise in fluorescence occurring at the edge. Transitions occurring at lower energies were fit using Gaussian functions, and the areas of the Gaussians were taken to be the peak areas.

For the EXAFS analysis, each data set was background-corrected and normalized. The data were converted to k space using the $k = [2m_e(E - E_o)/\hbar^2)]^{1/2}$ relationship, where m_e is the mass of the electron, $\hbar$ is Planck's constant divided by 2π, and E_o is the threshold energy of the absorption edge. The threshold energies chosen for the metals studied were 7723 eV for Co, 8340 eV for Ni, 8990 eV for Cu, and 9670 eV for Zn.[28] A Fourier transform of the data was produced using the data range k = 2−12.5 Å^{-1}, where the upper limit was determined by the signal:noise ratio. Scattering parameters for EXAFS fitting were generated using FEFF8.[31] The k^3-weighted data were fit in r space. The first coordination sphere was determined by setting the number of scattering atoms in each shell to integer values and systematically varying the combination of N/O and S donors (Tables S3−S22 of the Supporting Information).

Multiple-scattering parameters for imidazole ligands bound to various metals were generated from crystallographic coordinates using FEFF8 with previously published crystal structures as input.[17,31,33−36] The best fits resulted in four prominent multiple-scattering features, and paths with similar overall lengths were combined to make four imidazole scattering paths, matching these four prominent features as outlined by Costello et al.[37,38] The four combined paths were used to fit the data by setting the number of imidazole ligands per metal ion to integral values allowing r and σ^2 to vary.[37,38] This method of fitting imidazoles is an approximation; therefore, no physical label can be applied to these paths. To compare different models of the same data set, ifeffit utilizes three goodness of fit parameters: χ^2, reduced χ^2, and R factor. These parameters are not to be confused with nomenclature in which R is used for interatomic distance and χ for k space EXAFS. The statistical parameter, χ^2, that is minimized in a fit is given by eq 1

$$\chi^2 = \frac{N_{idp}}{N_{\varepsilon^2}} \sum_{N}^{i=1} (\{\mathrm{Re}[\tilde{\chi}_{data}(R_i) - \tilde{\chi}_{model}(R_i)]\}^2 + \{\mathrm{Im}[\tilde{\chi}_{data}(R_i) - \tilde{\chi}_{model}(R_i)]\}^2) \quad (1)$$

where N_{idp} is the number of independent data points, N_{ε^2} is the number of uncertainties to minimize, Re() denotes the real part of the EXAFS function, Im() is the imaginary part of the EXAFS fitting function, and $\tilde{\chi}(R_i)$ is the Fourier-transformed data or model function.

Reduced $\chi^2 = \chi^2/(N_{idp} - N_{varys})$, where N_{varys} is the number of refining parameters and represents the degrees of freedom in the fit. Additionally, ifeffit calculates the R factor for each fit, which is directly proportional to χ^2 and a measure of the absolute misfit between the data and theory. The R factor is given by eq 2 and is scaled to the magnitude of the data, making it proportional to χ^2.

$$R = \left[\sum_{i=1}^{N} (\{\mathrm{Re}[\tilde{\chi}_{data}(R_i) - \tilde{\chi}_{model}(R_i)]\}^2 + \{\mathrm{Im}[\tilde{\chi}_{data}(R_i) - \tilde{\chi}_{model}(R_i)]\}^2 \right) \Big/ \left[\sum_{i=1}^{N} (\{\mathrm{Re}[\tilde{\chi}_{data_i}(R_i)]\}^2 + \{\mathrm{Im}[\tilde{\chi}_{data}(R_i)]\}^2) \right] \quad (2)$$

In a comparison of different models, the R factor and reduced χ^2 parameter were used to determine which model was the best fit for the data. The R factor will always generally improve with an increasing number of adjustable parameters, while reduced χ^2 will go through a minimum and then increase, indicating that the model is overfitting the data.[39]

RESULTS

RcnR Metal Specificity in Vivo. The His → Cys mutations were tested for metal responsiveness using a *lacZ* reporter assay (Figure 2). The H60C and H67C mutant RcnR proteins show

dx.doi.org/10.1021/bi300886q | Biochemistry 2013, 52, 84−97

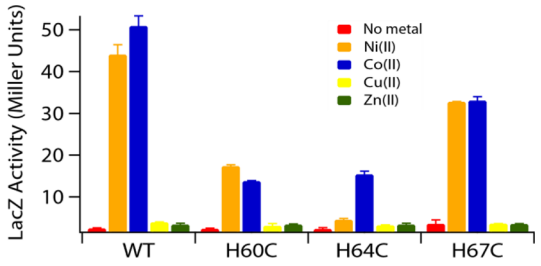

Figure 2. LacZ reporter assay showing the effect of the H60C-, H64C-, and H67C-RcnR mutations on the expression of P_{rcnA} in response to binding metal ions.

significant depression of P_{rcnA} transcription in response to addition of Ni(II) or Co(II). The H64C mutation was tested for metal responsiveness to Ni(II), Co(II), Cu(II), and Zn(II) (Figure 2); Cu(II) ions will be reduced to Cu(I) in the cytoplasm of the cell, as well as Cd(II) (Figure S2 of the Supporting Information).[40] Only in the presence of Co(II) was the H64C-RcnR mutant protein able to derepress P_{rcnA} transcription. Although several mutants have been previously characterized by Iwig et al.[24] that show a significant response to Ni(II) binding but not to Co(II) binding, this is the first mutant characterized to date that shows a significant response to binding Co(II) over binding Ni(II), and this is further evidence that the two cognate metals are recognized by distinct mechanisms.

XANES Analysis of H60C-, H64C-, and H67C-RcnR. Information regarding the coordination number and geometry of a metal center can be obtained by analyzing the XANES spectrum. XANES for H60C-, H64C-, and H67C-RcnR metal complexes are summarized in Table 1 and shown in Figure 3. Metals with a vacancy in the 3d manifold [e.g., Co(II) and Ni(II)] exhibit features in the XANES associated with bound transitions below the edge energy. These features include the 1s → 3d transition (with shake-down contributions), which is a measure of centrosymmetricity in the complex, and the peak associated with a 1s → $4p_z$ transition, which is present in tetragonal geometries lacking one or more axial ligands.

The Co(II) complexes of H60C-, H64C-, and H67C-RcnR proteins have a single pre-edge feature at ∼7710 eV (Table 1 and Figure 3) that is associated with the 1s → 3d transition. Like the WT protein,[24] the peak areas observed for the Co(II) protein complexes are larger than that of typical octahedral Co(II) complexes [0.069(8) eV][28] but smaller than that observed for five-coordinate complexes [0.220(3) eV].[29] The larger 1s → 3d peak areas observed for these Co(II) RcnR mutant protein complexes are consistent with a distorted octahedral geometry.[41] The Ni(II) complexes of H60C-, H64C-, and H67C-RcnR all have a relatively small peak associated with the 1s → 3d transition located at ∼8330 eV (Table 1 and Figure 3), suggesting that the ligand arrangements are centrosymmetric.[42] Only the spectrum obtained for H64C-RcnR and Ni(II) exhibits a small shoulder at ∼8338 eV, which corresponds to a 1s → $4p_z$ transition, consistent with either a distorted square-planar geometry or square-pyramidal geometry.[42] The presence of this small shoulder coupled with the small 1s → 3d peak area (0.016 eV) is most consistent with a distorted square-planar geometry.[42] The rest are therefore determined to be six-coordinate.

Cu(I) and Zn(II) complexes have no 1s → 3d transitions as they are d^{10} metals. For the Cu(I) complexes, there is a well-resolved 1s → 4p transition between 8983 and 8985 eV.[43] The shape, energy, and intensity of this peak can be used to determine the coordination geometry of the Cu(I) metal center.[43] The 1s → 4p transition in two-, three-, and four-coordinate model complexes have normalized absorption magnitudes of ∼1, ∼0.55, and between 0.6 and 0.9 at ∼8994, 8994, and 8995.5 eV, respectively.[43] H60C-, H64C-, and H67C-RcnR and WT RcnR[25] Cu(I) complexes have normalized intensities of 0.49, 0.48, 0.49, and 0.46, respectively, at ∼8984 eV. The intensity and energy of this peak suggest that the Cu(I) complexes are three-coordinate.

For Zn(II) complexes, information can be gained about the coordination number and geometry from the intensity and shape of the XANES spectra.[44,45] Information regarding the coordination number of the Zn(II) center can be determined by the intensity of the XANES as well as the relative position of the edge in energy.[45] The normalized intensity of what is termed the white line, the sharp intense peak arising from the absorption edge, increases with an increase in coordination number. For four-coordinate complexes, the normalized intensity of the white line is ∼1.3; five- and six-coordinate complexes have an intensity between 1.3 and 2, with six-coordinate being the most intense.[45] The edge energy for six-coordinate complexes is ∼2 eV higher than that of four- or five-coordinate complexes.[45] The XANES spectra for the WT Zn(II) complex is consistent with a four-coordinate complex,[25] whereas the edge energies and intensities of the Zn(II) complexes of H60C-, H64C-, and H67C-RcnR in buffer M with 300 mM NaBr are consistent with six-coordinate complexes for all three mutations. The corresponding Zn(II) complexes in buffer M with 300 mM NaOAc have edge energies that are more consistent with four- or five-coordinate Zn(II) complexes (∼9663 eV).[45]

EXAFS Analysis of H60C-, H64C-, and H67C-RcnR Complexes. EXAFS analysis provides information about the atomic number of scattering atoms ($Z \pm 2$), the distance between the absorbing and scattering atom (±0.02 Å in the first coordination sphere), and an estimate of the number of similar and distinct ligands (approximately ±20% for the total number of ligands).

H60C-RcnR. Table 1 and Figure 4 show the best fits for metal complexes of H60C-RcnR proteins in buffer M containing NaBr as well as the Zn(II) complex in buffer M with NaOAc. The best fits for the cognate metals, Ni(II) and Co(II), are six-coordinate, in agreement with the XANES analysis (vide supra), and the ligand environment is composed of five N/O donor ligands and one S donor ligand, as is the case for the WT protein.[24,25] Neither cognate metal picks up a second S donor ligand, nor do they bind anions (e.g., Br^-) from the buffer, suggesting that like WT-RcnR, all six ligands are derived from the protein.[24,25] The Ni(II) site structure in H60C-RcnR is essentially unaltered from the WT Ni(II) site structure, as both feature a long ∼2.61(2) Å Ni−S distance and one or two His imidazole ligands among five N/O donors with Ni−L distances of ∼2.1 Å. These results are consistent with the His60 side chain not being a ligand in the WT RcnR Ni(II) complex.

The Co(II) site fits best for two or three imidazole ligands; the tendency for an increase in the number of His ligands in the Co(II) complex relative to the Ni(II) complex is similar to that seen in the WT protein.[25] However, the Co(II) site in H60C-RcnR has a long 2.6 Å Co−S distance that is significantly altered from that of the Co(II) site in WT RcnR (2.3 Å) and more closely resembles that of the Ni(II) site in WT RcnR in

dx.doi.org/10.1021/bi300886q | Biochemistry 2013, 52, 84−97

Table 1. XANES and EXAFS Analysis for Metal Complexes of H60C-, H64C-, H67C-RcnR Mutant Proteins in Buffer with 300 mM NaBr[a]

	XANES analysis				EXAFS analysis					
metal ion	K-edge energy (eV)	1s → 3d peak area ($\times 10^2$ eV)	1s → $4p_z$ observed	coordination number	shell	r (Å)	σ^2 ($\times 10^{-3}$ Å^2)	ΔE_o (eV)	%R	reduced χ^2
				H60C-RcnR						
Co(II)	7720.6	13(3)	no	6	**5N/O (2Im)**	**2.13(1)**	**1.0(7)**	**0(2)**	**6.84**	**18.6**
					1S	**2.61(3)**	**4(3)**			
					5N/O (3Im)	2.13(1)	1.0(8)	0(2)	7.74	21.0
					1S	2.60(3)	4(4)			
Ni(II)	8343.7	5(1)	no	5/6	**5N/O (1Im)**	**2.080(7)**	**6.2(6)**	**11(1)**	**1.64**	**5.4**
					1S	**2.685(8)**	**1.0(7)**			
					5N/O (2Im)	2.079(7)	6.2(6)	10.4(9)	1.92	6.4
					1S	2.684(8)	0.9(7)			
Cu(I)	8987.3	NA	yes	3	**2N/O (1Im)**	**2.13(2)**	**2(2)**	**5(2)**	**2.56**	**10.0**
					1S	**2.33(9)**	**7(6)**			
					1Br	**2.50(3)**	**7(2)**			
					2N/O (2Im)	2.13(2)	1(2)	6(2)	2.57	10.1
					1S	2.36(7)	8(7)			
					1Br	2.49(2)	7(3)			
Zn(II)	9665.1	NA	NA	6	**3N/O (2Im)**	**2.00(3)**	**8(2)**	**−9(3)**	**2.01**	**17.9**
					2S	**2.36(3)**	**1(3)**			
					1Br	**2.33(3)**	**0.2(13)**			
					3N/O (3Im)	2.00(4)	8(3)	−10(4)	2.10	18.7
					2S	2.35(3)	0.3(29)			
					1Br	2.32(3)	0.1(15)			
Zn(II)[b]	9662.6	NA	NA	5	**3N/O (1Im)**	**2.04(1)**	**6.8(7)**	**−8(1)**	**0.51**	**4.0**
					2S	**2.297(6)**	**4.5(3)**			
					3N/O (2Im)	2.04(1)	6.7(8)	−8(1)	0.53	4.1
					2S	2.299(7)	4.5(4)			
				H64C-RcnR						
Co(II)	7721.0	9(1)	no	6	**3N/O (3Im)**	**2.02(2)**	**6(1)**	**−8(3)**	**1.27**	**5.6**
					2S	**2.33(3)**	**9(1)**			
					1Br	**2.67(3)**	**6(2)**			
					3N/O (2Im)	2.03(2)	6(1)	−8(3)	1.38	6.0
					2S	2.33(3)	9(2)			
					1Br	2.67(3)	6(2)			
Ni(II)	8343.9	1.6(9)	yes	4/5	**3N/O (3Im)**	**2.05(1)**	**3(1)**	**5(2)**	**2.63**	**7.7**
					1S	**2.31(3)**	**4(3)**			
					1Br	**2.69(5)**	**8(9)**			
					2N/O (2Im)	2.00(3)	3(3)	−3(4)	4.42	12.9
					1S	2.25(4)	0(2)			
					1Br	2.51(8)	6(6)			
Cu(I)	8987.1	NA	yes	3	**2N/O (1Im)**	**2.12(2)**	**2(3)**	**4(2)**	**2.18**	**8.5**
					1S	**2.32(6)**	**6(5)**			
					1Br	**2.50(2)**	**7(2)**			
Zn(II)	9664.5	NA	NA	6	**3N/O (3Im)**	**2.05(2)**	**4(2)**	**−5(3)**	**1.81**	**11.0**
					2S	**2.40(4)**	**1(3)**			
					1Br	**2.36(4)**	**1(2)**			
					3N/O (2Im)	2.06(2)	4(1)	−5(2)	1.82	11.1

dx.doi.org/10.1021/bi300886q | *Biochemistry* 2013, 52, 84−97

Table 1. continued

	XANES analysis				EXAFS analysis					
metal ion	K-edge energy (eV)	1s → 3d peak area ($\times 10^2$ eV)	1s → $4p_z$ observed	coordination number	shell	r (Å)	σ^2 ($\times 10^{-3}$ Å^2)	ΔE_o (eV)	%R	reduced χ^2
				H64C-RcnR						
					2S	2.41(3)	3(3)			
					1Br	2.38(3)	2(2)			
Zn(II)[b]	9662.7	NA	NA	5	**3N/O (3Im)**	**2.02(1)**	**7.0(9)**	**−9(2)**	**0.67**	**10.6**
					2S	**2.280(7)**	**3.8(4)**			
					3N/O (2Im)	2.02(1)	7(1)	−9(2)	0.75	11.9
					2S	2.279(7)	3.8(4)			
				H67C-RcnR						
Co(II)	7720.8	13(2)	no	6	**3N/O**	**2.07(2)**	**2(1)**	**−4(2)**	**2.13**	**5.2**
					2N/O (3Im)	**2.20(2)**	**0(2)**			
					1S	**2.63(1)**	**1(1)**			
					3N/O	2.07(2)	2(2)	−3(2)	2.18	5.3
					2N/O (2Im)	2.20(2)	0(2)			
					1S	2.63(1)	1(1)			
Ni(II)	8343.3	5(1)	no	5/6	5N/O (3Im)	2.05(1)	2.1(9)	5(2)	6.81	98.0
					1S	2.7(1)	5(11)			
					5N/O (2Im)	**2.06(1)**	**2(1)**	**6(2)**	**7.15**	**102.9**
					1S	**2.62(8)**	**6(8)**			
Ni(II)[b]	8343.1	3(1)	no	6	**5N/O (2Im)**	**2.083(6)**	**3.8(5)**	**9(1)**	**2.23**	**16.3**
					1S	**2.67(2)**	**4(2)**			
					5N/O (3Im)	2.083(7)	3.8(5)	9(1)	2.55	16.5
					1S	2.67(2)	4(2)			
					5N/O (1Im)	2.083(7)	3.8(5)	9(1)	2.27	16.6
					1S	2.67(2)	3(2)			
Cu(I)	8984.9	NA	yes	3	**1N/O (1Im)**	**2.04(3)**	**0(3)**	**5(5)**	**5.45**	**45.4**
					1S	**2.31(5)**	**3(3)**			
					1Br	**2.51(2)**	**3(2)**			
Zn(II)	9665.0	NA	NA	6	**4N/O**	**2.15(2)**	**6(1)**	**5(2)**	**2.63**	**26.2**
					1N/O (2Im)	**1.90(4)**	**14(4)**			
					1S	**2.69(4)**	**8(5)**			
					4N/O	2.14(2)	5(1)	4(2)	2.64	26.3
					1N/O (3Im)	1.90(4)	14(5)			
					1S	2.69(6)	11(8)			
Zn(II)[b]	9663.6	NA	NA	4	**2N/O (1Im)**	**1.981(8)**	**3.6(6)**	**−9(1)**	**0.61**	**13.6**
					2S	**2.271(7)**	**6.0(4)**			
					2N/O (2Im)	1.980(9)	3.6(6)	−9(1)	0.61	13.7
					2S	2.271(8)	6.0(4)			

[a]The numbers in parentheses are the estimated uncertainties in the corresponding variables. These uncertainties are calculated by SixPack and reflect the change in the variable that will result in an increase in χ^2 of 1. EXAFS fits in bold type are shown in Figures 4−6. [b]Sample prepared in buffer with 20 mM Hepes, 300 mM NaOAc, and 10% glycerol (pH 7.0).

this respect.[24,25] Although the data cannot unambiguously differentiate Cys35 from Cys60 as the source of the S donor ligand, the fact that Co(II), Ni(II), Cu(I), and Zn(II) ions all bind to Cys35 in the WT protein[25] and other mutants in which the Co(II) site features the long M−S distance have been characterized (e.g., H3C-RcnR and H3E-RcnR)[25] is consistent with the S donor present being Cys35. Nonetheless, it is not clear whether the structure changed because of the loss of His60 as a ligand or as a result of another structural change in the metal site (e.g., loss of an H-bond) that results in Co(II) occupying a site that more closely resembles the WT RcnR Ni(II) site. Because one might expect that the mutation would result in the loss of one His ligand and feature two Cys S donors if His60 were a Co(II) ligand, the result is more

dx.doi.org/10.1021/bi300886q | Biochemistry 2013, 52, 84−97

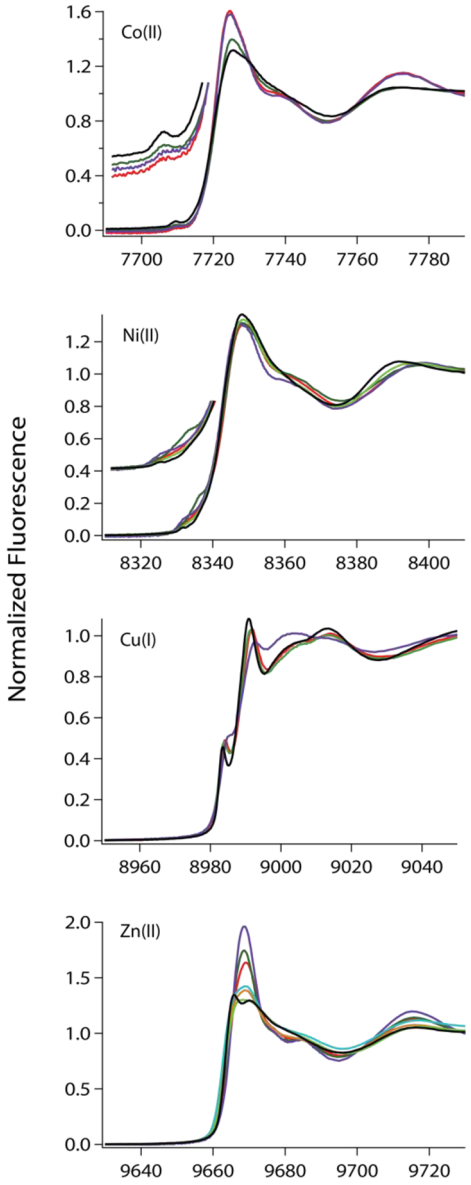

Figure 3. XANES spectra of metal complexes of RcnR proteins in buffer with 20 mM Hepes, 300 mM NaBr, and 10% glycerol: H60C (red), H64C (dark green), H67C (purple), and WT from ref 25 (black). XANES spectra in buffer with 300 mM NaOAc instead of NaBr: H60C (orange), H64C (aqua), and H67C (light green).

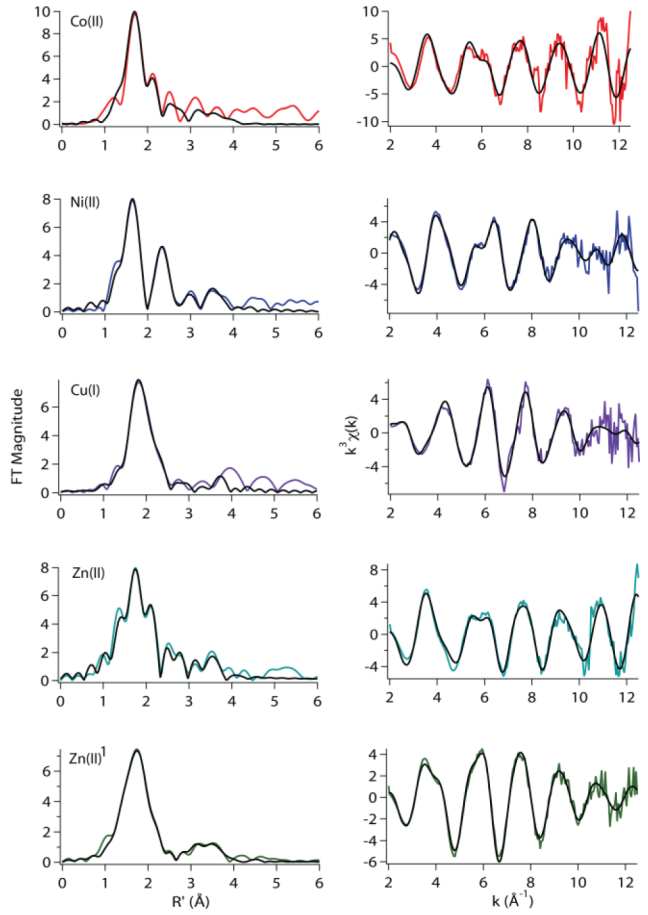

Figure 4. K-Edge XAS spectra of H60C-RcnR metal complexes in buffer containing 20 mM Hepes, 300 mM NaBr/[1]NaOAc, and 10% glycerol (pH 7.0). For Cu(I), the buffer also contained 2 mM TCEP: (left) Fourier-transformed EXAFS data (colored lines) and fits (black lines) and (right) unfiltered k^3-weighted EXAFS spectra and fits.

consistent with a role for His60 as a secondary coordination sphere residue involved in stabilizing the WT Co(II) conformation of the protein. The *lacZ* assay data (vide supra) show that the protein is still responsive to both Co(II) and Ni(II) binding. This is probably due to the fact that both metals adopt a geometry and a ligand set that is similar to that of binding of Ni(II) to WT RcnR and therefore supports a role for His60 in stabilizing the Co(II) conformation as seen in the WT RcnR Co(II) complex.[24]

The structures of the noncognate metal ions, Cu(I) and Zn(II), show dramatically different responses to the H60C mutation in RcnR. A four-coordinate Cu(I) complex forms with H60C-RcnR that is composed of a $(N/O)_2SBr$ ligand donor atom set that incorporates a bromide from the buffer. As in the Co(II) and Ni(II) complexes of H60C-RcnR, the metal does not bind to two S donors. The ligands involved in the H60C-RcnR Cu(I) complex are identical to those seen for the Cu(I) complex of WT RcnR; the M−L distances are similar [for WT-RcnR, Cu−N = 2.13(2) Å, Cu−S = 2.291(7) Å, and Cu−Br = 2.62(1) Å].[25] The similarity of these structures indicates that His60 is not a ligand involved in the binding of Cu(I) to WT-RcnR. According to the EXAFS analysis, the coordination number of the Cu(I) center is four, a result that is inconsistent with the XANES analysis (vide supra) that predicts a three-coordinate Cu(I) site (Table 1 and Figure 3). A similar discrepancy is observed in the analysis of data from the WT RcnR Cu(I) complex.[25] It is possible that the long (weak) interactions with Br^- are not enough to alter the XANES features to indicate a four-coordinate site.

In contrast to the Ni(II), Co(II), and Cu(I) complexes of H60C-RcnR, the best fit for the H60C-RcnR Zn(II) complex shows that both Cys residues are ligands. Additionally, the data obtained for the Zn(II) site indicate that the Zn(II) is coordinated by three N/O donors, of which two or three are imidazoles, and a bromide ligand, making the complex six-coordinate, in agreement with the XANES analysis (vide supra). This contrasts with the four-coordinate tetrahedral $Zn[(N/O)_2SBr]$ complex found for the WT RcnR Zn(II) complex.[25] Although six-coordinate Zn(II) sites are unusual,[46] they are not unprecedented in RcnR mutants. In a series of His3 mutations, the H3L mutation has no effect on the Zn(II) site, and the H3C mutation results in a five-coordinate Zn[(N/

dx.doi.org/10.1021/bi300886q | *Biochemistry* 2013, 52, 84−97

$O)_2S_2Br]$ that becomes a six- or seven-coordinate (with a bidentate carboxylate) $Zn[(N/O)_6S]$ site in H3E-RcnR and confers Zn sensing capability to the protein.[25] Although His3 is clearly not a ligand for the WT RcnR Zn(II) site, the site displays an ability to accommodate additional ligands and to change coordination number. The coordination number of the Zn(II) complexes of H60C-RcnR also shows some unusual sensitivity to the nature of the anions present in the buffer. The Zn(II) complex of H60C-RcnR is six-coordinate in buffer M with NaBr but five-coordinate in buffer M with NaOAc (Table 1). The H60C-RcnR Zn(II) in buffer M with NaBr fits best for three N/O donors at an average distance of 2.00 Å, of which two or three are imidazoles, two S donord at 2.35 Å, and a Br^- ligand at 2.33 Å. The lengths determined for the Zn−S and Zn−Br bonds are almost indistinguishable. For this reason, the data were also taken in buffer M with NaOAc. The EXAFS data from the Zn(II) H60C protein in buffer M with NaOAc (Figure 4) fit best for three N/O donors at 2.04 Å, of which one or two are imidazoles, and two S donors at 2.30 Å. The sample in NaOAc buffer yielded a similar fit sans the Br^- ligand, confirming that the protein did, in fact, bind both sulfurs present in the H60C protein.

H64C-RcnR. The His64 residue of RcnR corresponds to a cysteine residue in *M. tuberculosis* CsoR, Cys65 (Figure 1), and this cysteine residue is a key ligand used to coordinate Cu(I) in CsoR.[17] The Co(II) complex of H64C-RcnR is shown by XANES analysis to be six-coordinate, and EXAFS analysis is consistent with this. The EXAFS analysis shows more than one change in metal site structure occurs for this mutation. The Co(II) site is composed of three N/O donors, of which two or three are histidines, at an average distance of 2.02 Å, two S donors at an average distance of 2.33 Å, and one Br^- ligand at 2.67 Å (Table 1 and Figure 5). The fit is similar in buffer with NaCl except that a Cl^- ligand is bound instead of a Br^- ligand (Table S10 of the Supporting Information). This mutation resulted in binding of the Cys64 residue, which is consistent with His64 being a ligand in the WT RcnR Co(II) complex, but also opened a coordination site on Co(II) that is occupied by an exogenous buffer ligand. The analysis cannot identify the N/O donor ligand that is lost, and the reason for the loss is not clear. However, changing a protein ligand from an imidazole to a thiolate will affect the electronic structure of the metal, which can influence the strength of the interaction with other ligands.

In contrast to the Co(II) site in H64C RcnR, the best fit for the Ni(II) EXAFS data is five-coordinate with three histidine ligands at an average distance of 2.05 Å, one S donor at 2.31 Å, and a Br^- ligand at 2.69 Å (Table 1 and Figure 5). [There is also a four-coordinate fit that is similar with the exception that there is one fewer histidine ligand and the Ni−S bond distance is shorter, consistent with a four-coordinate nickel center.[47] However, the five-coordinate fit improves both %*R* and reduced χ^2 by 40%. A similar result was observed for this sample in buffer with NaCl (Table S12 of the Supporting Information), where the five-coordinate EXAFS fit improves %*R* and reduced χ^2 by 12% (Table S12 of the Supporting Information).] Whether the site has a distorted four- or five-coordinate geometry, the data show a major disruption of the WT RcnR Ni(II) site structure that is at least consistent with the involvement of His64 as a Ni(II) ligand. The structure obtained for the mutant protein involves a short Ni−S bond that is comparable to the Co−S distance that is found in WT RcnR,[24,25] but it is not clear which of the two Cys residues is involved, particularly given the large number of structural changes involved.

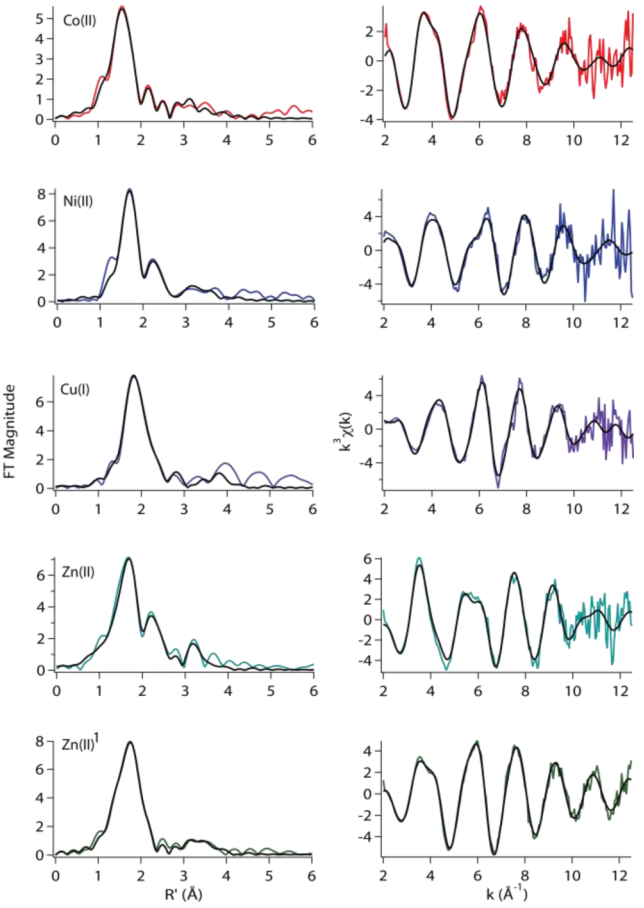

Figure 5. K-Edge XAS spectra of H64C-RcnR metal complexes in buffer containing 20 mM Hepes, 300 mM NaBr/[1]NaOAc, and 10% glycerol (pH 7.0). For Cu(I), the buffer also contained 2 mM TCEP: (left) Fourier-transformed EXAFS data (colored lines) and fits (black lines) and (right) unfiltered k^3-weighted EXAFS spectra and fits.

The complexes formed with H64C-RcnR and noncognate metal ions, Cu(I) and Zn(II), are similar to those formed by the H60C mutation, suggesting that His64 may be a ligand of Zn(II) but is clearly not a ligand for Cu(I). EXAFS analysis for the Cu(I) sample reveals that the Cu(I) site is four-coordinate and binds the exogenous buffer ligand similar to that seen for the H60C-RcnR Cu(I) complex and in WT RcnR.[25] However, the H64C-RcnR Cu(I) complex in buffer with NaCl (Table S14 of the Supporting Information) indicates that the best fit for the data is three-coordinate with two N/O donors at 2.10 Å and one S donor at 2.36 Å. The appearance of Br^-, but not Cl^-, in the coordination sphere of Cu(I) was also noted in the WT RcnR Cu(I) complex[25] and is not surprising considering the facts that Cu(I) often occupies three-coordinate sites and is also a softer acid and would thus have a higher affinity for Br^- than for Cl^-.

Like the H60C-RcnR Zn(II) protein, the Zn(II) site in the H64C-RcnR protein is also six-coordinate in buffer M with NaBr and five-coordinate in buffer with NaOAc (Table 1), the difference between the two fits being that the sample in buffer M with NaBr has an additional Br^- ligand derived from the buffer. The H64C-RcnR Zn(II) complex formed in buffer M with NaBr is coordinated by three N/O ligands at an average

dx.doi.org/10.1021/bi300886q | *Biochemistry* 2013, 52, 84−97

distance of 2.05 Å, of which two or three are imidazoles, two S donors at 2.40 Å, and a Br^- ligand at 2.36 Å.

H67C-RcnR. The XANES and EXAFS analysis are in agreement for the cognate metals, which feature six-coordinate sites (Table 1). As in H60C-RcnR, the Co(II) site resembles the Ni(II) site in that the Co(II) metal ion is coordinated by a S donor ligand at 2.63 Å. The best fit for the Co(II) site also includes two shells of N/O donors, three at an average distance of 2.07 Å and two at an average distance of 2.20 Å, of which two or three are imidazoles (Table 1 and Figure 6). The Ni(II) site fits best for five N/O donors at an average distance of 2.06 Å, of which two are imidazoles, and a S donor at 2.62 Å. The corresponding fit involving three imidazoles results in an improvement in both %*R* and reduced χ^2; however, the error for the sulfur bond distance is larger, and for this reason, the sample was repeated in buffer M containing NaOAc. The best fit for this data is five N/O donors, of which two are imidazoles, and a S donor ligand, a result that is indistinguishable from that for the WT RcnR Ni(II) site structure.[25]

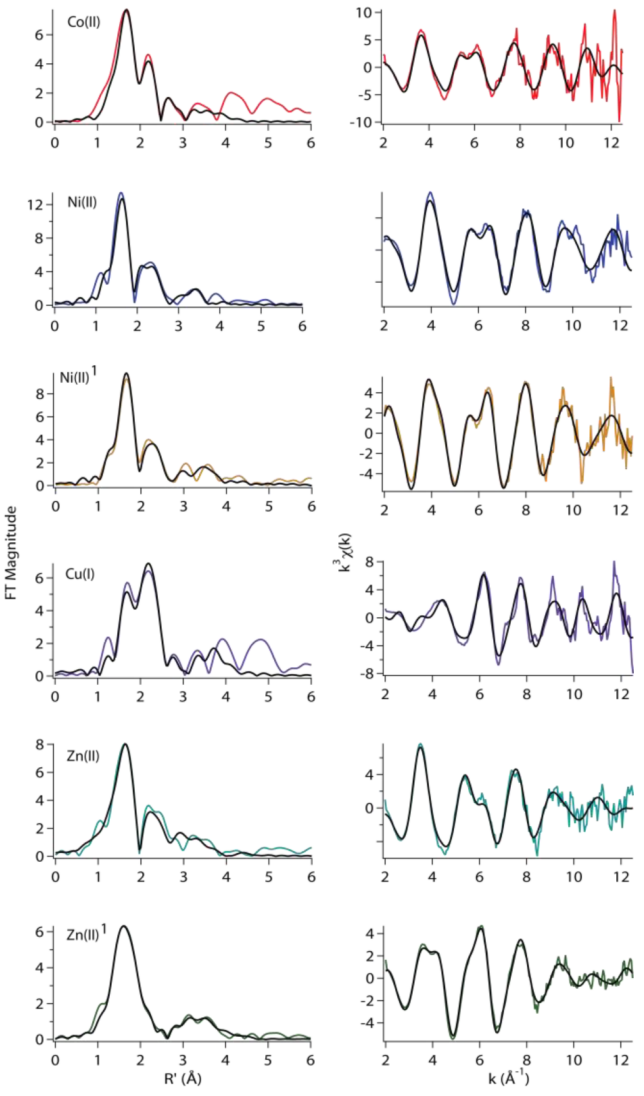

Figure 6. K-Edge XAS spectra of H67C-RcnR metal complexes in buffer containing 20 mM Hepes, 300 mM NaBr/[1]NaOAc, and 10% glycerol (pH 7.0). For Cu(I), the buffer also contained 2 mM TCEP: (left) Fourier-transformed EXAFS data (colored lines) and fits (black lines) and (right) unfiltered k^3-weighted EXAFS spectra and fits.

The Cu(I) site in H67C-RcnR is three-coordinate, in agreement with the XANES analysis. The site is coordinated by a histidine ligand at 2.04 Å, a S donor at 2.31 Å, and a Br^- at 2.51 Å. The Cu(I) is still coordinated by an exogenous buffer ligand but differs from the H60C- and H64C-RcnR Cu(I) samples in that it binds one fewer N/O donor. Thus, His67 is either a ligand of the Cu(I) complex or necessary for the positioning of another amino acid side chain to coordinate Cu(I). The Zn(II) site shows some variability based on buffer selection. The sample in buffer with NaBr (Table 1 and Figure 6) is a six-coordinate $Zn[(N/O)_5S]$ site, with a Zn−S distance of 2.27 Å. As such, it resembles the WT RcnR Co(II) site structure. However, in buffer containing NaOAc, the Zn(II) ion adopts a four-coordinate $Zn[(N/O)_2S_2]$ structure that coordinates both Cys residues present in the protein, consistent with H67 being a ligand in the four-coordinate site. This is the fourth example of the coordination number of a metal site in an RcnR protein being influenced by the nature of the anion bound, and the first example of an alteration of protein ligand selection by the metal center. For Cu(I), the metal is often four-coordinate with bromide present but is three-coordinate in alternate buffers, without an obvious alteration in the three remaining ligands.

DISCUSSION

Metalloregulator function depends upon a selective response to binding by a cognate metal ion. Selectivity is generally elicited by requiring a coordination geometry that is favored by the cognate metal and disfavored by noncognate metals. The ramifications of the RcnR His to Cys mutations for metal site structures provide further insight into the role of specific His ligands in complexes formed with cognate and noncognate metal ions and show that in some cases, a Co(II) response may be observed when the Co(II) ion adopts a structure similar to that of the WT RcnR Ni(II) site.

Cognate Metal Complexes. The results presented here, along with those obtained previously,[24,25] collectively suggest that His3, His60, His64, and His67 are potential Co(II) ligands. Histidine coordination appears to be less important for Ni(II) binding, as only His64 has been clearly shown to be important for the six-coordinate Ni(II) site. The precise roles of His60 and His67 in the WT RcnR Co(II) complex are obscured by the fact that the H60C and H67C mutations lead to Co(II) site structures that resemble the WT RcnR Ni(II) complex[24,25] and do not introduce an additional S ligand. Thus, it is possible that His60 and His67 play allosteric roles that stabilize a unique protein structure that gives rise to the WT RcnR Co(II) complex. Alternatively, because the mutation affects the chemical identity of the side chain, the potential for main chain coordination cannot currently be excluded. These results are in general agreement with those from a mutational survey by Iwig et al.,[24] based on the loss of transcriptional response in *lacZ* reporter assays. Those studies showed that His3 and His64 are important for response to both Ni(II) and Co(II) bound to WT RcnR, and His60 mutations impair only the Co(II) response.[24] His3 was later shown using XAS to be a ligand in the Co(II) complex, but not in the Ni(II) complex, suggesting an allosteric role for His3 in the Ni(II) complex.[25]

Functional studies conducted by Iwig et al.[24] showed that when His60 was mutated to Ala, Asn, Leu, and Arg, all of the mutations resulted in a loss of Co(II)-responsive transcriptional

dx.doi.org/10.1021/bi300886q | *Biochemistry* 2013, 52, 84−97

regulation by RcnR. However, only H60R-RcnR resulted in a loss of responsiveness for both cognate metals [Ni(II) and Co(II)], with the remaining mutations resulting in proteins that were still Ni(II)-responsive, demonstrating that the His60 side chain was not essential for response to Ni(II)-specific function. For the H60C mutation studied here, RcnR retains a response to both cognate metals. However, the structural information available from XAS analysis shows that this is not due simply to the swap of one protein ligand (His) for another (Cys), because neither cognate metal ion coordinates an additional S donor ligand. The structure of the Ni(II) site is not perturbed by the mutation, indicating that His60 is not a ligand in the Ni(II) site, and in agreement with expectations from the prior mutagenesis studies.[24] However, the Co(II) site structure is altered in H60C-RcnR. Although it also does not show ligation of both Cys residues, the structure features the long Co−S distance that is reminiscent of the M−S distance seen in the WT RcnR Ni(II) site,[24,25] but not in the WT RcnR Co(II) site. On the basis of studies of the N-terminus of the protein that showed that differential recognition of Co(II) versus Ni(II) involved His3 as a ligand only in the case of Co(II), as well as the different M−S distances, a model that involved different protein conformations in the two complexes was developed to explain differential recognition of Co(II) and Ni(II). Other mutants involving His3 were found to bind Co(II), but with metric parameters that closely resembled those of the WT RcnR Ni(II) site.[25] Many of these mutants had residual responses to Co(II) ions. The H60C-RcnR mutant protein may be responsive to Co(II) because it is recognizing the ion by the same mechanism that WT RcnR recognizes Ni(II).

When His64 was mutated to Leu, it eliminated Co(II) response but only slightly impaired Ni(II) responsiveness,[24] suggesting a scenario similar to that described above for the His60 mutations. However, the H64C mutation results in the first example of an RcnR protein that retains a significant response to Co(II) but lacks a response to binding Ni(II) (Figure 2). The XAS studies show that the H64C-RcnR Co(II) site resembles the Co(II) site in WT RcnR[25] with substitution of a His64 ligand by the additional Cys ligand, including maintenance of the 2.3 Å Co−S distance. This is the result expected for a simple ligand substitution, producing a protein that is able to maintain the six-coordinate structure of the WT RcnR complex, and thus its response to Co(II) binding. Therefore, His64 may play a role in Co(II) binding in RcnR similar to that of His86 and His100 in the Zn(II)-responsive transcriptional regulator in *Staphylococcus aureus* CzrA. CzrA binds Zn(II) in a tetrahedral geometry with three histidines and one aspartate (His86, His97, His100, and Asp84).[48] Mutagenesis studies coupled with DNA binding and UV−vis studies [using the Co(II) protein] revealed that Asp84 and His97 are necessary to maintain tetrahedral geometry and Zn(II)-mediated regulation. Mutations of these residues resulted in metal binding in non-native geometries that did not support allosteric coupling of metal and DNA binding.[49] However, His86 and His100 are necessary for Zn(II) binding, but metal binding residues like Asp, Glu, Asn, and Gln were shown to coordinate Zn(II) in a tetrahedral environment and mediate DNA binding.[49] Like His86 and His100 in CzrA, His64 in RcnR is necessary for Co(II) binding, and mutating His64 to another metal binding residue such as Cys maintains an octahedral geometry for the Co(II) site necessary for mediating the regulation of binding of RcnR to DNA.

In the case of Ni(II), the H64C-RcnR binding site is disrupted in the complex in a way that does not maintain the Ni−S distance in the WT RcnR structure, does not incorporate a second Cys ligand, and opens the site to exogenous anion binding. This mutation changes the Ni(II) site from six-coordinate in the case of WT RcnR[24,25] to four- or five-coordinate with the loss of at least two protein ligands and the addition of an exogenous buffer ligand, suggesting that His64, like the N-terminus,[25] is necessary for maintaining a six-coordinate Ni(II) site. The H64C mutation results in a loss of Ni(II) response but provides no further insight into the role of His64 as a Ni(II) ligand, which could be part of an allosteric network that maintains the conformation of the protein in the Ni(II) complex.

Finally, His67 has also been previously mutated to Leu, which had no effect on the responsiveness to either of the cognate metals. This result is also seen for the H67C-RcnR mutation reported here. However, XAS structural analysis shows that the Co(II) ion adopts a structure similar to the WT RcnR Ni(II) site structure (M−S distance of ∼2.6 Å),[25] indicating that the Co(II) response is being maintained in H67C-RcnR by the mechanism used to generate a response to Ni(II) binding. Although the results do not prove a role for His67 as a Co(II) ligand, His67 must at least play a role in stabilizing the Co(II) site structure in WT RcnR, either as a ligand or through H-bonding interactions that stabilize the protein structure. His67 is not conserved in RcnR proteins and is predicted to be in a loop region, based on structural homology with CsoR.

Noncognate Metal Complexes. The effect of the His60, His64, and His67 residues on the structures of the noncognate metal ions reveals that these residues have distinctive roles in binding noncognate metals. These sites overlap with the cognate metal binding sites, for example, in the use of Cys35 as a ligand, but in some cases, His ligands that are involved in binding noncognate metals are not involved in binding the cognate metals. This suggests that the sites occupied by noncognate metals may prevent these metals from binding to some of the ligands adopted by cognate metals (e.g., the N-terminal amine).

Cu(I). The Cu(I) complexes with the His → Cys mutants are either three- or four- coordinate, depending upon whether a buffer anion is bound. Even with the additional Cys residue added by the H60C-, H64C-, and H67C-RcnR mutant proteins, the Cu(I) site does not resemble that of Cu(I)-bound CsoR, which has a coordination environment involving one His ligand and two S donors.[17] The Cu(I) complex of H60C-RcnR has a structure that is very much like that of the WT RcnR Cu(I) complex[25] and does not bind the second Cys residue available in this mutant. Thus, His60 is likely not a ligand for the RcnR Cu(I) complex. Similarly, the Cu(I) site in H64C-RcnR is unaffected by the mutation and is similar to that seen for the Cu(I) complex of WT RcnR[25] and H60C-RcnR. The complex formed by Cu(I) and H67C-RcnR is distinct from those of the H60C and H64C mutants. The coordination number decreases from four in the other mutants (including bromide) to three with the loss of one His ligand. Thus, His67 is identified as a ligand for Cu(I). On the basis of the $His_2(Cys)$ Br ligand set seen in the WT RcnR Cu(I) complex in buffer M with NaBr,[25] the only ligand in common with the WT RcnR Ni(II) site is the single Cys35 ligand. Interestingly, Cu(I) never bound a $His(Cys)_2$ ligand set like that of found in the CsoR

dx.doi.org/10.1021/bi300886q | *Biochemistry* 2013, 52, 84−97

Cu(I) complex, even when presented with the identical CsoR ligand set in H64C-RcnR.

Zn(II). The situation for Zn(II) is more complex. In buffer M containing NaBr, all three His → Cys mutants are six-coordinate and therefore presumably occupy a six-coordinate site that is more similar to the WT RcnR Co(II) and Ni(II) sites than to the WT Zn(II) site. The cognate metals both utilize His64, and Co(II) may also bind to His60 (vide supra). The Zn(II) complexes of H60C- and H64C-RcnR show the formation of a six-coordinate $(N/O)_3S_2Br$ complex in buffer M with NaBr, consistent with these residues being ligands in the six-coordinate site. The Zn−S distance is 2.40 Å, so the site most closely resembles the WT RcnR Co(II) site and is very similar to the $(N/O)_3S_2Br$ Co(II) site in the H64C-RcnR mutant. In buffer M with NaOAc, the bromide ligands are not present and five-coordinate $(N/O)_3S_2$ complexes are observed.

The complex formed by H67C-RcnR with Zn(II) is distinct from the other His mutants. In buffer M with NaBr, the $(N/O)_5S$ complex formed is six-coordinate but features only a single S donor and has no bromide ligand. The Zn−S distance is long [2.69(4) Å], and thus, this site most closely resembles the WT RcnR Ni(II) site. However, in buffer M with NaOAc, Zn(II) adopts a four-coordinate $(N/O)_2S_2$ site, where Cys67 is a ligand, consistent with His67 being a ligand in the four-coordinate WT RcnR Zn(II) site. However, this possibility cannot be distinguished from simple displacement of the bromide ligand found in the WT RcnR $(N/O)_2SBr$ site by the additional cysteinate ligand.

Distinct Mechanisms for Metal Recognition by Orthologs RcnR and CsoR. The results of this and previous studies[24,25] indicate that besides coordination number and ligand selection, there is a key difference between the molecular mechanisms that couple metal recognition to allosteric response in the RcnR/CsoR family of transcriptional regulators. Only two of the Cu(I) binding residues in CsoR are conserved in RcnR, Cys36 and His61 (using *M. tuberculosis* CsoR numbering). Additionally, in RcnR proteins, there is a conserved His residue at position 3. This residue corresponds to Glu4 in *M. tuberculosis* CsoR. On the basis of the *M. tuberculosis* CsoR crystal structure, Glu4 is positioned close to the CsoR Cu(I) binding site.[17] Prior studies of RcnR have established that cognate metal binding to the N-terminal amine and the interaction with His3 are key determinants in the mechanism of metal recognition by RcnR that apparently play no role in CsoR Cu(I) binding.[24,25]

None of the RcnR His → Cys mutants studied here confer any response to either Cu(I) or Zn(II), including H64C-RcnR, where the residues are identical to those in the Cu(I) binding site of CsoR or adopt the Cu(I) site structure found in that protein. As seen in InrS,[23] simply having the first-coordination sphere residues present necessary for Cu(I) binding (as seen in CsoR) is not sufficient to elicit Cu(I) responsiveness.[17,50] The CsoR Cu(I) structure reveals that there is a hydrogen bonding network involving metal-binding residue His61 as well as Tyr35 and Glu81. Work done by Ma et al. determined that this hydrogen bonding network is important in allosterically coupling metal binding with DNA binding in CsoR.[50] Even if Cu(I) were to bind H64C-RcnR with $His(Cys)_2$ coordination, as in CsoR, it is likely the protein would not show a change in DNA binding affinity because the protein lacks the second-coordination sphere residues needed to couple metal binding with DNA binding.[17,50] These data indicate that while the secondary, tertiary, and quaternary structures of CsoR and RcnR are similar, the specific mechanisms for metal ion recognition are quite different and small changes in primary sequence account for changes not just in coordination geometry but also in the allosteric network of residues required for a functional response.

The H60C-, H64C-, and H67C-RcnR mutants with Zn(II) all feature six-coordinate Zn(II) sites. However, binding of Zn(II) to these mutant proteins does not result in the derepression of P_{rcnA} transcription. Thus, the mere formation of a six-coordinate Zn(II) site is not sufficient to provide a transcriptional response, despite the one observed for the Zn(II) complex of H3E-RcnR.[25] Although Zn(II) adopts the correct geometry in the H60C-, H64C-, and H67C-RcnR mutations, they apparently do not allow the Zn(II) ion to bind the N-terminus of RcnR and therefore cannot drive the necessary conformational changes required to disfavor RcnR−DNA binding interactions.

The identification of Cu(I)- and Zn(II)-coordinating residues in RcnR, combined with the different allosteric networks utilized by RcnR and CsoR, suggests that the metal specificity of RcnR could be reengineered via judicious mutations that promote Cu(I) or Zn(II) binding but not Ni(II) or Co(II) binding. Additional directed mutations in the N-terminus of RcnR would be required to ensure binding produces a functional response. This has already been observed in Zn(II)-substituted H3E-RcnR,[25] which offers promise for additional successful engineering.

■ ASSOCIATED CONTENT

Supporting Information

Table of mutagenic primers used for the H60C, H64C, and H67C mutants, EPR spectra of H60C-, H64C-, and H67C-RcnR Cu(I) complexes and Cu(II)-EDTA, *lacZ* reporter assay of H64C-RcnR, and tables with additional XAS fits for wild-type and mutant RcnR proteins. This material is available free of charge via the Internet at http://pubs.acs.org.

■ AUTHOR INFORMATION

Corresponding Author

*Phone: (413) 545-6876. E-mail: mmaroney@chemistry.umass.edu.

Present Addresses

[‖]Department of Chemistry, Indiana University, Bloomington, IN 47405.

[⊥]Department of Chemistry and Biochemistry, Oberlin College, Oberlin, OH 44074.

Funding

This work was supported by National Institutes of Health (NIH) Grant R01-GM069696 to M.J.M. and National Science Foundation Grant MCB0520877 to P.T.C. XAS data collection at the National Synchrotron Light Source at Brookhaven National Laboratory was supported by the U.S. Department of Energy, Division of Materials Sciences and Division of Chemical Sciences. Beamline X3B at NSLS is supported by the NIH. This publication was made possible by Center for Synchrotron Biosciences Grant P30-EB-009998 from the National Institute of Biomedical Imaging and Bioengineering. Portions of this research were conducted at the Stanford Synchrotron Radiation Light (SSRL) source, a national user facility operated by Stanford University on behalf of the U.S. Department of Energy, Office of Basic Energy Sciences. The SSRL Structural Molecular Biology Program is supported by

the Department of Energy, Office of Biological and Environmental Research, and by the National Institutes of Health, National Center for Research Resources, Biomedical Technology Program.

Notes

The authors declare no competing financial interest.

■ ABBREVIATIONS

amp, ampicillin; cam, chloramphenicol; CsoR, copper-sensitive operon repressor; EPR, electron paramagnetic resonance; EXAFS, extended X-ray absorption fine structure; Hyp, hydrogenase pleiotropy; H_2ase, hydrogenase; InrS, internal nickel-responsive sensor; ICP-OES, inductively coupled plasma optical emission spectroscopy; IPTG, isopropyl β-D-1-thiogalactopyranoside; NikR, nickel-responsive regulator of the *nik* operon; RcnR, resistance to cobalt and nickel repressor; TCEP, tris(2-carboxyethyl)phosphine hydrochloride; XANES, X-ray absorption near-edge spectroscopy; XAS, X-ray absorption spectroscopy.

■ REFERENCES

(1) Rosenzweig, A. C. (2002) Metallochaperones: Bind and deliver. *Chem. Biol. 9*, 673−677.
(2) Pennella, M. A., and Giedroc, D. P. (2005) Structural determinants of metal selectivity in prokaryotic metal-responsive transcriptional regulators. *BioMetals 18*, 413−428.
(3) Böck, A., King, P. W., Blokesch, M., and Posewitz, M. C. (2006) Maturation of hydrogenases. *Adv. Microb. Physiol. 51*, 1−71.
(4) Forzi, L., and Sawers, R. G. (2007) Maturation of [NiFe]-hydrogenases in *Escherichia coli*. *BioMetals 20*, 565−578.
(5) De Pina, K., Navarro, C., McWalter, L., Boxer, D. H., Price, N. C., Kelly, S. M., Mandrand-Berthelot, M. A., and Wu, L. F. (1995) Purification and characterization of the periplasmic nickel-binding protein NikA of *Escherichia coli* K12. *Eur. J. Biochem. 227*, 857−865.
(6) Navarro, C., Wu, L. F., and Mandrand-Berthelot, M. A. (1993) The nik operon of *Escherichia coli* encodes a periplasmic binding-protein-dependent transport system for nickel. *Mol. Microbiol. 9*, 1181−1191.
(7) Atanassova, A., and Zamble, D. B. (2005) *Escherichia coli* HypA is a zinc metalloprotein with a weak affinity for nickel. *J. Bacteriol. 187*, 4689−4697.
(8) Mehta, N., Olson, J. W., and Maier, R. J. (2003) Characterization of *Helicobacter pylori* nickel metabolism accessory proteins needed for maturation of both urease and hydrogenase. *J. Bacteriol. 185*, 726−734.
(9) Zhang, J. W., Butland, G., Greenblatt, J. F., Emili, A., and Zamble, D. B. (2005) A role for SlyD in the *Escherichia coli* hydrogenase biosynthetic pathway. *J. Biol. Chem. 280*, 4360−4366.
(10) Leach, M. R., Sandal, S., Sun, H., and Zamble, D. B. (2005) Metal binding activity of the *Escherichia coli* hydrogenase maturation factor HypB. *Biochemistry 44*, 12229−12238.
(11) Rodrigue, A., Effantin, G., and Mandrand-Berthelot, M. A. (2005) Identification of rcnA (yohM), a nickel and cobalt resistance gene in *Escherichia coli*. *J. Bacteriol. 187*, 2912−2916.
(12) Koch, D., Nies, D. H., and Grass, G. (2007) The RcnRA (YohLM) system of *Escherichia coli*: A connection between nickel, cobalt and iron homeostasis. *BioMetals 20*, 759−771.
(13) Blériot, C., Effantin, G., Lagarde, F., Mandrand-Berthelot, M. A., and Rodrigue, A. (2011) RcnB is a periplasmic protein essential for maintaining intracellular Ni and Co concentrations in *Escherichia coli*. *J. Bacteriol. 193*, 3785−3793.
(14) De Pina, K., Desjardin, V., Mandrand-Berthelot, M. A., Giordano, G., and Wu, L. F. (1999) Isolation and characterization of the nikR gene encoding a nickel-responsive regulator in *Escherichia coli*. *J. Bacteriol. 181*, 670−674.
(15) Chivers, P. T., and Sauer, R. T. (1999) NikR is a ribbon-helix-helix DNA-binding protein. *Protein Sci. 8*, 2494−2500.
(16) Iwig, J. S., Rowe, J. L., and Chivers, P. T. (2006) Nickel homeostasis in *Escherichia coli*: The rcnR-rcnA efflux pathway and its linkage to NikR function. *Mol. Microbiol. 62*, 252−262.
(17) Liu, T., Ramesh, A., Ma, Z., Ward, S. K., Zhang, L., George, G. N., Talaat, A. M., Sacchettini, J. C., and Giedroc, D. P. (2007) CsoR is a novel *Mycobacterium tuberculosis* copper-sensing transcriptional regulator. *Nat. Chem. Biol. 3*, 60−68.
(18) Ma, Z., Jacobsen, F. E., and Giedroc, D. P. (2009) Coordination chemistry of bacterial metal transport and sensing. *Chem. Rev. 109*, 4644−4681.
(19) Iwig, J. S., and Chivers, P. T. (2009) DNA recognition and wrapping by *Escherichia coli* RcnR. *J. Mol. Biol. 393*, 514−526.
(20) Blaha, D., Arous, S., Bleriot, C., Dorel, C., Mandrand-Berthelot, M. A., and Rodrigue, A. (2011) The *Escherichia coli* metallo-regulator RcnR represses rcnA and rcnR transcription through binding on a shared operator site: Insights into regulatory specificity towards nickel and cobalt. *Biochimie 93*, 434−439.
(21) Sakamoto, K., Agari, Y., Agari, K., Kuramitsu, S., and Shinkai, A. (2010) Structural and functional characterization of the transcriptional repressor CsoR from *Thermus thermophilus* HB8. *Microbiology 156*, 1993−2005.
(22) Dwarakanath, S., Chaplin, A. K., Hough, M. A., Rigali, S., Vijgenboom, E., and Worrall, J. A. (2012) Response to Copper Stress in *Streptomyces lividans* Extends beyond Genes under Direct Control of a Copper-sensitive Operon Repressor Protein (CsoR). *J. Biol. Chem. 287*, 17833−17847.
(23) Foster, A. W., Patterson, C. J., Pernil, R., Hess, C. R., and Robinson, N. J. (2012) Cytosolic Ni(II) sensor in cyanobacterium: Nickel detection follows nickel affinity across four families of metal sensors. *J. Biol. Chem. 287*, 12142−12151.
(24) Iwig, J. S., Leitch, S., Herbst, R. W., Maroney, M. J., and Chivers, P. T. (2008) Ni(II) and Co(II) sensing by *Escherichia coli* RcnR. *J. Am. Chem. Soc. 130*, 7592−7606.
(25) Higgins, K. A., Chivers, P. T., and Maroney, M. J. (2012) Role of the N-terminus in determining metal-specific responses in the *E. coli* Ni- and Co-responsive metalloregulator, RcnR. *J. Am. Chem. Soc. 134*, 7081−7093.
(26) Ma, Z., Cowart, D. M., Scott, R. A., and Giedroc, D. P. (2009) Molecular insights into the metal selectivity of the copper(I)-sensing repressor CsoR from *Bacillus subtilis*. *Biochemistry 48*, 3325−3334.
(27) Thompson, J. D., Higgins, D. G., and Gibson, T. J. (1994) CLUSTAL W: Improving the sensitivity of progressive multiple sequence alignment through sequence weighting, position-specific gap penalties and weight matrix choice. *Nucleic Acids Res. 22*, 4673−4680.
(28) Leitch, S., Bradley, M. J., Rowe, J. L., Chivers, P. T., and Maroney, M. J. (2007) Nickel-specific response in the transcriptional regulator, *Escherichia coli* NikR. *J. Am. Chem. Soc. 129*, 5085−5095.
(29) Padden, K. M., Krebs, J. F., MacBeth, C. E., Scarrow, R. C., and Borovik, A. S. (2001) Immobilized metal complexes in porous organic hosts: Development of a material for the selective and reversible binding of nitric oxide. *J. Am. Chem. Soc. 123*, 1072−1079.
(30) Webb, S. M. (2005) SIXpack: A graphical user interface for XAS analysis using IFEFFIT. *Phys. Scr. T115*, 1011−1014.
(31) Ankudinov, A. L., Ravel, B., Rehr, J. J., and Conradson, S. D. (1998) Real-space multiple-scattering calculation and interpretation of X-ray-absorption near-edge structure. *Phys. Rev. B 58*, 7565−7576.
(32) Zabinsky, S. I., Rehr, J. J., Ankudinov, A., Albers, R. C., and Eller, M. J. (1995) Multiple-scattering calculations of X-ray-absorption spectra. *Phys. Rev. B: Condens. Matter Mater. Phys. 52*, 2995−3009.
(33) Guncar, G., Wang, C. I., Forwood, J. K., Teh, T., Catanzariti, A. M., Ellis, J. G., Dodds, P. N., and Kobe, B. (2007) The use of Co^{2+} for crystallization and structure determination, using a conventional monochromatic X-ray source, of flax rust avirulence protein. *Acta Crystallogr. F63*, 209−213.
(34) Chivers, P. T., and Tahirov, T. H. (2005) Structure of *Pyrococcus horikoshii* NikR: Nickel sensing and implications for the regulation of DNA recognition. *J. Mol. Biol. 348*, 597−607.

(35) Crane, B. R., Di Bilio, A. J., Winkler, J. R., and Gray, H. B. (2001) Electron tunneling in single crystals of *Pseudomonas aeruginosa* azurins. *J. Am. Chem. Soc. 123*, 11623−11631.
(36) Gasper, R., Scrima, A., and Wittinghofer, A. (2006) Structural insights into HypB, a GTP-binding protein that regulates metal binding. *J. Biol. Chem. 281*, 27492−27502.
(37) Costello, A., Periyannan, G., Yang, K. W., Crowder, M. W., and Tierney, D. L. (2006) Site-selective binding of Zn(II) to metallo-β-lactamase L1 from *Stenotrophomonas maltophilia*. *J. Biol. Inorg. Chem. 11*, 351−358.
(38) Costello, A. L., Sharma, N. P., Yang, K. W., Crowder, M. W., and Tierney, D. L. (2006) X-ray absorption spectroscopy of the zinc-binding sites in the class B2 metallo-β-lactamase ImiS from *Aeromonas veronii* bv. sobria. *Biochemistry 45*, 13650−13658.
(39) Herbst, R. W., Guce, A., Bryngelson, P. A., Higgins, K. A., Ryan, K. C., Cabelli, D. E., Garman, S. C., and Maroney, M. J. (2009) Role of conserved tyrosine residues in NiSOD catalysis: A case of convergent evolution. *Biochemistry 48*, 3354−3369.
(40) Giedroc, D. P., and Arunkumar, A. I. (2007) Metal sensor proteins: Nature's metalloregulated allosteric switches. *Dalton Trans.*, 3107−3120.
(41) Wirt, M. D., Sagi, I., Chen, E., Frisbie, S. M., Lee, R., and Chance, M. R. (1991) Geometric Conformations of Intermediates of B_{12} Catalysis by X-Ray Edge Spectroscopy: Co(I) B_{12}, Co(II) B_{12}, and Base-Off Adenosylcobalamin. *J. Am. Chem. Soc. 113*, 5299−5304.
(42) Colpas, G. J., Maroney, M. J., Bagyinka, C., Kumar, M., Willis, W. S., Suib, S. L., Baidya, N., and Mascharak, P. K. (1991) X-Ray Spectroscopic Studies of Nickel-Complexes, with Application to the Structure of Nickel Sites in Hydrogenases. *Inorg. Chem. 30*, 920−928.
(43) Kau, L. S., Spirasolomon, D. J., Pennerhahn, J. E., Hodgson, K. O., and Solomon, E. I. (1987) X-ray Absorption-Edge Determination of the Oxidation-State and Coordination-Number of Copper: Application to the Type-3 Site in Rhus-Vernicifera Laccase and Its Reaction with Oxygen. *J. Am. Chem. Soc. 109*, 6433−6442.
(44) Clark-Baldwin, K., Tierney, D. L., Govindaswamy, N., Gruff, E. S., Kim, C., Berg, J., Koch, S. A., and Penner-Hahn, J. E. (1998) The limitations of X-ray absorption spectroscopy for determining the structure of zinc sites in proteins. When is a tetrathiolate not a tetrathiolate? *J. Am. Chem. Soc. 120*, 8401−8409.
(45) Jacquamet, L., Aberdam, D., Adrait, A., Hazemann, J. L., Latour, J. M., and Michaud-Soret, I. (1998) X-ray absorption spectroscopy of a new zinc site in the fur protein from *Escherichia coli*. *Biochemistry 37*, 2564−2571.
(46) Kuppuraj, G., Dudev, M., and Lim, C. (2009) Factors governing metal-ligand distances and coordination geometries of metal complexes. *J. Phys. Chem. B 113*, 2952−2960.
(47) Jenkins, R. M., Singleton, M. L., Almaraz, E., Reibenspies, J. H., and Darensbourg, M. Y. (2009) Imidazole-containing (N_3S)-Ni(II) complexes relating to nickel containing biomolecules. *Inorg. Chem. 48*, 7280−7293.
(48) Eicken, C., Pennella, M. A., Chen, X., Koshlap, K. M., VanZile, M. L., Sacchettini, J. C., and Giedroc, D. P. (2003) A metal-ligand-mediated intersubunit allosteric switch in related SmtB/ArsR zinc sensor proteins. *J. Mol. Biol. 333*, 683−695.
(49) Pennella, M. A., Arunkumar, A. I., and Giedroc, D. P. (2006) Individual metal ligands play distinct functional roles in the zinc sensor *Staphylococcus aureus* CzrA. *J. Mol. Biol. 356*, 1124−1136.
(50) Ma, Z., Cowart, D. M., Ward, B. P., Arnold, R. J., DiMarchi, R. D., Zhang, L., George, G. N., Scott, R. A., and Giedroc, D. P. (2009) Unnatural amino acid substitution as a probe of the allosteric coupling pathway in a mycobacterial Cu(I) sensor. *J. Am. Chem. Soc. 131*, 18044−18045.